Analytical Glycobiology

Identification and characterization of *O*-linked glycans in cervical mucus as biomarkers of sperm transport: A novel sheep model

Laura Abril-Parreño [iD][2,3]**, Hayden Wilkinson**[4,5]**, Anette Krogenæs**[6]**, Jack Morgan**[4]**, Mary E Gallagher**[7]**, Colm Reid**[7]**, Xavier Druart**[8]**, Sean Fair**[1,2,†]**, and Radka Saldova**[1,4,5,9,†]

[2]Laboratory of Animal Reproduction, Department of Biological Sciences, School of Natural Sciences, Biomaterials Research Cluster, Bernal Institute, Faculty of Science and Engineering, University of Limerick, V94 T9PX Limerick, Ireland, [3]Teagasc, Animal & Grassland Research and Innovation Centre, C15 PW93 Grange, Ireland, [4]NIBRT GlycoScience Group, The National Institute for Bioprocessing Research and Training, Blackrock, A94 X099 Dublin, Ireland, [5]CÚRAM, SFI Research Centre for Medical Devices, National University of Ireland, H91 W2TY Galway, Ireland, [6]Faculty of Veterinary Medicine, Department of Production Animal Clinical Sciences, Norwegian University of Life Sciences, 5003 1432 Ås, Norway, [7]Veterinary Sciences Centre, University College Dublin, D04 W6F6 Belfield, Ireland, [8]UMR-PRC, INRA-85, Université de Tours, IFCE, Physiologie de la Reproduction et des Comportements, Institut National de la Recherche Agronomique, 37380 Nouzilly, France, and [9]School of Medicine, College of Health and Agricultural Science, University College Dublin, D07 A8NN Dublin 4, Ireland

To whom correspondence should be addressed: Radka Saldova, Tel: +35 312158147; Fax: +353 1 215 8116; e-mail: radka.fahey@nibrt.ie; Sean Fair, Tel: +353 61 202548; e-mail: sean.fair@ul.ie
[†]Both authors contributed equally.

Abstract

Cervical mucus plays an important role in female fertility, since it allows the entry of motile and morphological normal sperm while preventing the ascent of pathogens from the vagina. The function of cervical mucus is critically linked to its rheological properties that are in turn dictated by *O*-glycosylated proteins, called mucins. We aimed to characterize the *O*-glycan composition in the cervical mucus of six European ewe breeds with known differences in pregnancy rates following cervical/vaginal artificial insemination with frozen–thawed semen, which are due to reported differences in cervical sperm transport. These were Suffolk (low fertility) and Belclare (medium fertility) in Ireland, Ile de France and Romanov (both with medium fertility) in France, and Norwegian White Sheep (NWS) and Fur (both with high fertility) in Norway ($n = 28$–30 ewes/breed). We identified 124 *O*-glycans, from which 51 were the major glycans with core 2 and fucosylated glycans as the most common structures. The use of exogenous hormones for synchronization did not affect the *O*-glycan composition in both high-fertility ewe breeds, but it did in the other four ewe breeds. There was a higher abundance of the sulfated glycan (Galβ1–3[SO3-GlcNAcβ1–6]GalNAc), fucosylated glycan (GlcNAcβ1–3(Fucα1–2Galβ1–3)GalNAc) and core 4 glycan (GlcNAcβ1–3[GlcNAcβ1–6]GalNAc) in the low-fertility Suffolk breed compared with NWS (high fertility). In addition, core 4 glycans were negatively correlated with mucus viscosity. This novel study has identified *O*-glycans that are important for cervical sperm transport and could have applications across a range of species including human.

Introduction

In vaginal depositors such as humans and sheep, hundreds of millions to billions of spermatozoa are deposited into the vagina with a small percentage of these entering the cervix and uterus, whereas only a few hundred spermatozoa are thought to arrive at the site of fertilization in the ampulla. During this long and tortuous journey, spermatozoa encounter a number of physiological barriers, the first of which is the cervix. Cervical goblet epithelial cells secrete large quantities of cervical mucus, which is a viscoelastic fluid that allows the entry of sperm to the upper genital tract while also preventing ascending pathogens from the vagina. In the lead up to ovulation when levels of estrogen are high, mucus production and hydration increase, whereas mucus viscosity is decreased (Gipson et al. 2001). This is essential to allow motile and morphologically normal sperm reach the site of fertilization (Katz et al. 1980; Ragni et al. 1985). Therefore, sperm migration through the cervix is dependent on the cervical mucus properties, including mucus volume, viscosity and biochemical composition.

The key component of cervical mucus are mucins, high molecular weight glycoproteins that exhibit a complex molecular structure (Lagow et al. 1999). Mucins comprise hydrophobic, partially folded termini and a polyanionic, highly glycosylated, and elongated protein core (Corfield 2015). *O*-glycans constitute the main component of mucins and confer a hydrophilic characteristic by binding water through hydrogen bonds, which increases mucus hydration (Marczynski et al. 2020). Proteomic analysis has identified differences in *O*-glycosylation across the phases of the menstrual cycle (Andersch-Bjorkman et al. 2007), where in humans around the time of ovulation there were more neutral fucosylated structures than in the pre- or postovulatory phases. Mucin gene expression has also been examined, showing a peak of mucin production around the time of ovulation, which also promotes mucus hydration (Gipson 2001) and sperm migration (Ma et al. 2016). Mucus structure also changes during the estrous cycle as preovulatory mucus is arranged in a dense filamentous structure like a net of interconnected fibers, whereas ovulatory mucus consists of dispersed floating globules of aggregated mucin molecules, which allow sperm migration through the mucus mesh around the time of ovulation (Brunelli et al. 2007; Lai et al. 2009). In addition, the sperm glycocalyx is rich in glycans with sialic acids as terminal monosaccharides, which typically interact with terminal sugars of the cervical mucins. For example, *N*-acetyl glucosamine on the sperm surface showed high affinity for sialic acid of the cervical mucus (Tecle and Gagneux 2015; Ma et al. 2016). Therefore, *O*-glycans in the cervical mucus are important modulators of not only mucus viscosity but also mediate biochemical interactions with sperm.

The ewe is an excellent model for investigating how spermatozoa are selected in the female reproductive tract as semen is deposited vaginally and cervical artificial insemination (AI) is limited due to poor pregnancy rates when frozen–thawed semen is used. Worldwide, pregnancy rates rarely exceed 30% when frozen–thawed semen is used in conjunction with cervical AI. However, Norway is the exception to this, since they routinely achieve pregnancy rates of 60–70% with vaginal (shot-in-the-dark) AI to a natural estrous (Paulenz et al. 2005). Previous studies by our group have demonstrated that this is due to the breed of the ewe used in Norway and specifically the inability of frozen–thawed sperm to traverse the cervix of some ewe breeds (Donovan et al. 2004; Fair et al. 2005). These ewe breed differences are not due to the gross anatomy of the cervix, the amount of mucus produced or its viscosity (Abril-Parreno et al. 2020) or differences in the periovulatory endocrine profiles between breeds (Fair et al. 2007, 2019). In a recent study, we found fewer sperm in the cervical crypts of Suffolk ewes (low fertility) compared with Belclare ewes (high fertility), which was associated with higher sialic acid content in the cervix of Suffolk ewes compared with Belclare ewes (Richardson et al. 2019). This suggests that large mucin *O*-glycans may cause the attachment of frozen–thawed sperm to the cervical mucus, thus impeding sperm migration through the cervix in some ewe breeds.

Therefore, the objective of this study was to characterize the *O*-glycans in cervical mucus around the time of ovulation of both a synchronized and natural cycle in six European ewe breeds known to have differences in pregnancy rates following cervical AI with frozen–thawed semen. Detailed and quantitative comparisons of *O*-glycan structures between ewe breeds with known differences in sperm transport may help to identify novel biomarkers of sperm transport, which is applicable across a wide range of species, including human.

Results

Most prevalent *O*-glycans in follicular phase cervical mucin

Representative chromatograms of each ewe breed are shown in Figure 1, outlining the main glycans identified across 51 major integrated peaks (full peak annotation in Supplementary Figure S1). From those, the five glycans with highest average area included: GlcAβ1–3/4Galβ1–3[SO3-Neu5Gcα2–6]GalNAc (peak 36), core 2 glycan Galα1–3Galβl1–3[Galα1–3GlcNAcβ1–6]GalNAc (peak 35), core 2 glycan Galβ1–3[Galβ1–4GlcNAcβ1–6]GalNAc (peak 24), core 1 glycan Galβ1–3GalNAc (peak 4), core 2 fucosylated and sulfated glycan GlcAβ1–3/4(Fucα1–2galβ1–3)[SO3-Neu5Gcα2–6]GalNAc (peak 37) (from highest to lowest average area under the curve, respectively). Peeling peaks were not included in this ranking as they are degradation products of the chemical method to release the *O*-glycans.

Combining fluorescence hydrophilic interaction ultra-performance liquid chromatography (FLR-HILIC-UPLC), exoglycosidase digestions and electrospray ionization mass spectrometry (ESI-MS) for assignment confirmation, our structural analyses identified 124 *O*-glycans in total across a range of mucin-type cores (Supplementary Table SII). Core 2 glycans were the most common structures with a 45.2% of the total, followed by core 1 glycans (21.8%), core 6 (10.5%), core 4 (6.5%) and core 3 (5.6%); graphical representations of each core type are shown in Figure 2. Of these structures, there were 56 (37.8%) fucosylated glycans, 37 (25%) sialylated (19 Neu5Ac type and 18 Neu5Gc type), 22 (14.9%) sulfated and 21 (14.2%) glycans contained terminal α-galactose epitopes (with an additional three capped by sialic acid). In addition, 73 (49.3%) *O*-glycans contained a terminal galactose epitope (both α- and β-linked) and five (3.4%) structures
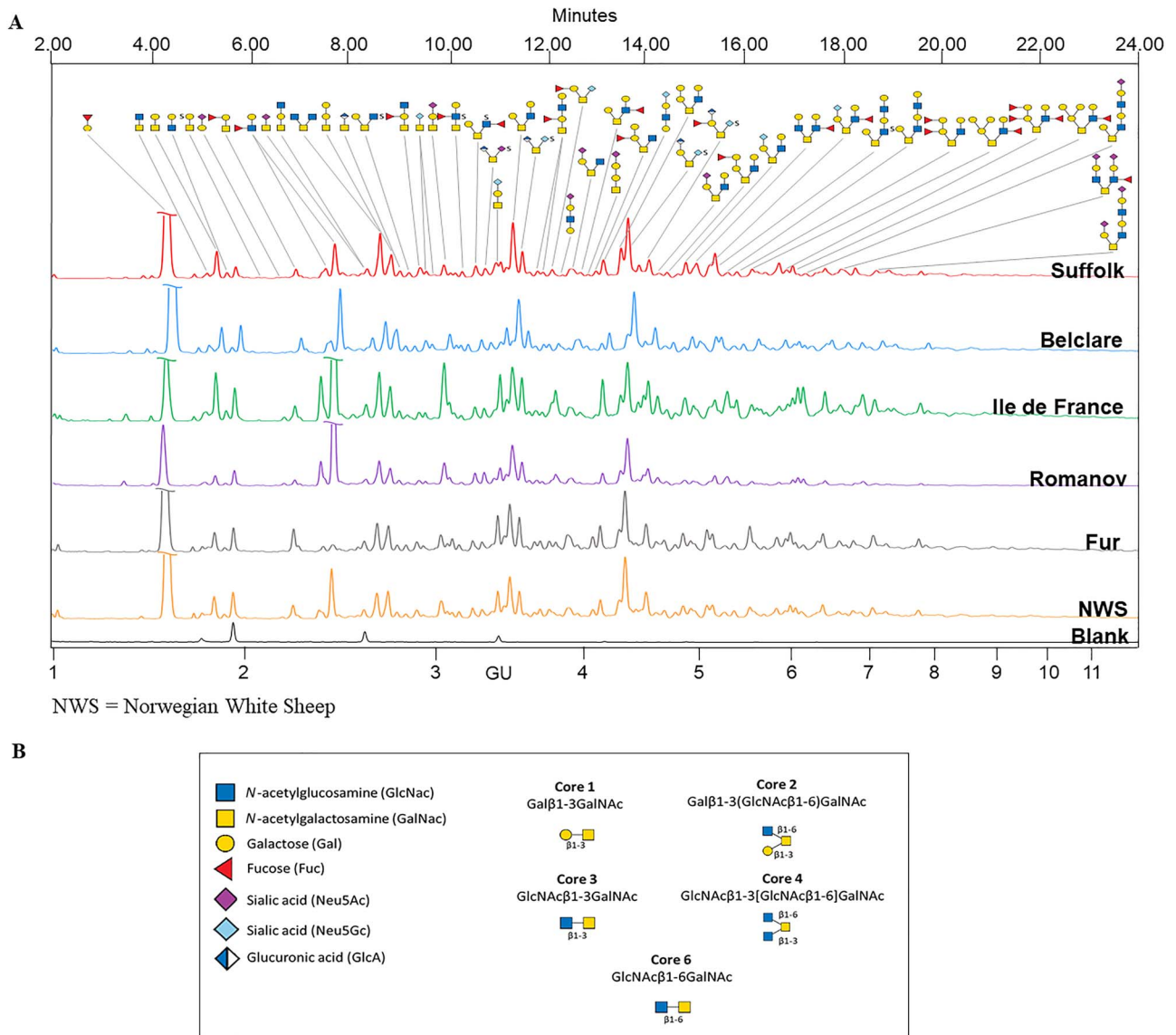
Fig. 1. (A) Representative FLR-HILIC-UPLC chromatograms of O-glycans released by microwave-assisted nonreductive β-elimination in sheep follicular phase cervical mucin (six European ewe breeds ordered top-down from lowest to highest fertility). Blank in black. Retention times of all identified glycan peaks expressed in glucose units (GUs). Major components of each peak shown. **(B)** Structural symbols for the O-glycans and common core structures found in this study.

contained an uncommon glucuronic acid terminal epitope. A total of 21 (14.2%) peeling products were additionally identified (full list including MS confirmation in Supplementary Table SIII). Exoglycosidase arrays used to identify these structures are presented in Supplementary Tables SIV–SIX. In addition, released N-glycans were analyzed using FLR-HILIC-UPLC; however, we did not identify N-glycan peaks.

Differences in cervical mucin O-glycan content collected at the follicular phase between a natural and a synchronized estrous cycle

Individual glycan peaks were compared across the six ewe breeds at both the natural and synchronized estrous cycles to identify significant cycle-related differences. We identified a ewe breed by type of cycle interaction ($P < 0.05$; Table I) represented by

differences between synchronization and natural cycle for some ewe breeds but not others. In the Suffolk breed (low fertility), type 3 H-antigen (Fucα1–2Galβ1–3)GalNAc (peak 8) and glucuronyl-Tn-antigen GlcAβ1–3GalNAc (peak 14) were higher in the natural cycle compared with the synchronized cycle ($P < 0.05$). In the medium fertility ewe breeds, Belclare had four glycans with higher expression at the natural than at the synchronized cycle (Neu5Acα2–3GalNAc and GlcNAcβ1–3Galβ1–3GalNAc (both in peak 11) 11; Galα1–3Galβ1–3GalNAc (peak 13) and a fucosylated glycan (Galβ1–3GlcNAcβ1–3(Fucα1–2Galβ1–3)GalNAc (peak 26)) ($P < 0.05$). In Ile de France, core 1 T-antigen Galβ1–3GalNAc (peak 4) and Galβ1–3GlcNAc (peak 5) were increased at the natural cycle ($P < 0.05$). However, a fucosylated glycan GlcNAcβ1–3(Fucα1–2Galβ1–3)GalNAc (peak 16) was decreased at the natural compared with the synchronized cycle ($P < 0.05$). In Romanov ewes, T-antigen (peak 4) was increased at the natural cycle ($P < 0.05$), whereas
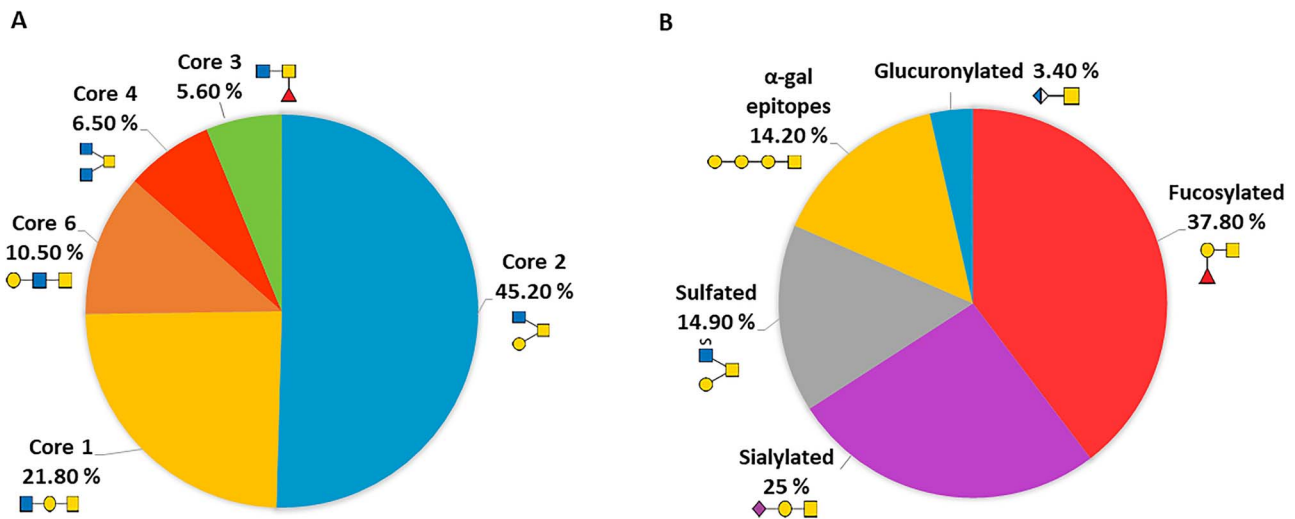
A

B

Fig. 2. Pie charts showing the relative abundance of (**A**) of the core glycan types and (**B**) the main types of glycan modifications in sheep cervical mucins at the follicular phase, including pictograms of representative structures of each type of core and modification, respectively.

Table I. Cervical mucus *O*-glycans that were significantly different at the follicular phase of a natural and synchronized cycle in six European ewe breeds

Major component of Peak		Peak	Natural vs. Synchronized (P value)					
			Suffolk	Belclare	Ile de France	Romanov	Fur	NWS
Galβ1-3GalNAc		4	0.052	0.103	0.001	0.001	1.000	0.147
Galβ1-3GlcNAc		5	0.276	1.000	0.020	0.116	0.976	0.587
(Fucα1-2Galβ1-3)GalNAc		8	0.012	0.521	0.659	1.000	1.000	0.159
Neu5Acα2-3GalNAc and GlcNAcβ1-3Galβ1-3GalNAc		11	1.000	0.903	1.000	0.006	0.245	1.000
Galα1-3Galβ1-3GalNAc		13	0.270	0.024	1.000	1.000	0.973	0.649
GlcAβ1-3GalNAc		14	0.002	0.287	0.810	1.000	0.922	0.867
GlcNAcβ1-3(Fucα1-2Galβ1-3)GalNAc		16	1.000	1.000	0.049	0.999	1.000	1.000
Galβ1-3GlcNAcβ1-3(Fucα1-2Galβ1-3)GalNAc		26	0.996	0.020	1.000	0.977	0.136	0.985

NWS = Norwegian White Sheep

Green indicates a significant increase of that particular glycan in the natural cycle and red indicates a significant decrease of that particular glycan in the natural cycle. Only *O*-glycans with significant differences are shown ($P < 0.05$). NWS = Norwegian White Sheep.

sialyl-Tn antigen (Neu5Acα2–3GalNAc) and GlcNAcβ1–3Galβ1–3GalNAc (both in peak 11) were decreased ($P < 0.05$). There were no differences in the two Norwegian ewe breeds between natural and synchronized cycles ($P > 0.05$).

Variation in the glycan profile between ewe breeds under the effect of synchronization were further categorized by feature (total fucosylation, total *N*-acetylneuraminic sialic acid (Neu5Ac), *N*-glycolylneuraminic sialic acid (Neu5Gc), sulfation, glucuronylation, type of core and peeling) to determine the significant trends. The only feature differences in this analysis were an overall upregulation of total core 1 structures in Belclare ewe breed at the natural cycle ($P < 0.001$; Supplementary Table SX), arising from upregulated Neu5Acβ2–3GalNAc and GlcNAcβ1–3Galβ1–3GalNAc ($P < 0.05$; peak 11), Galα1–3Galβ1–3GalNAc ($P < 0.05$; peak 13), and Galβ1–3GlcNAcβ1–3(Fucα1–2Galβ1–3)GalNAc ($P < 0.05$; peak 26).
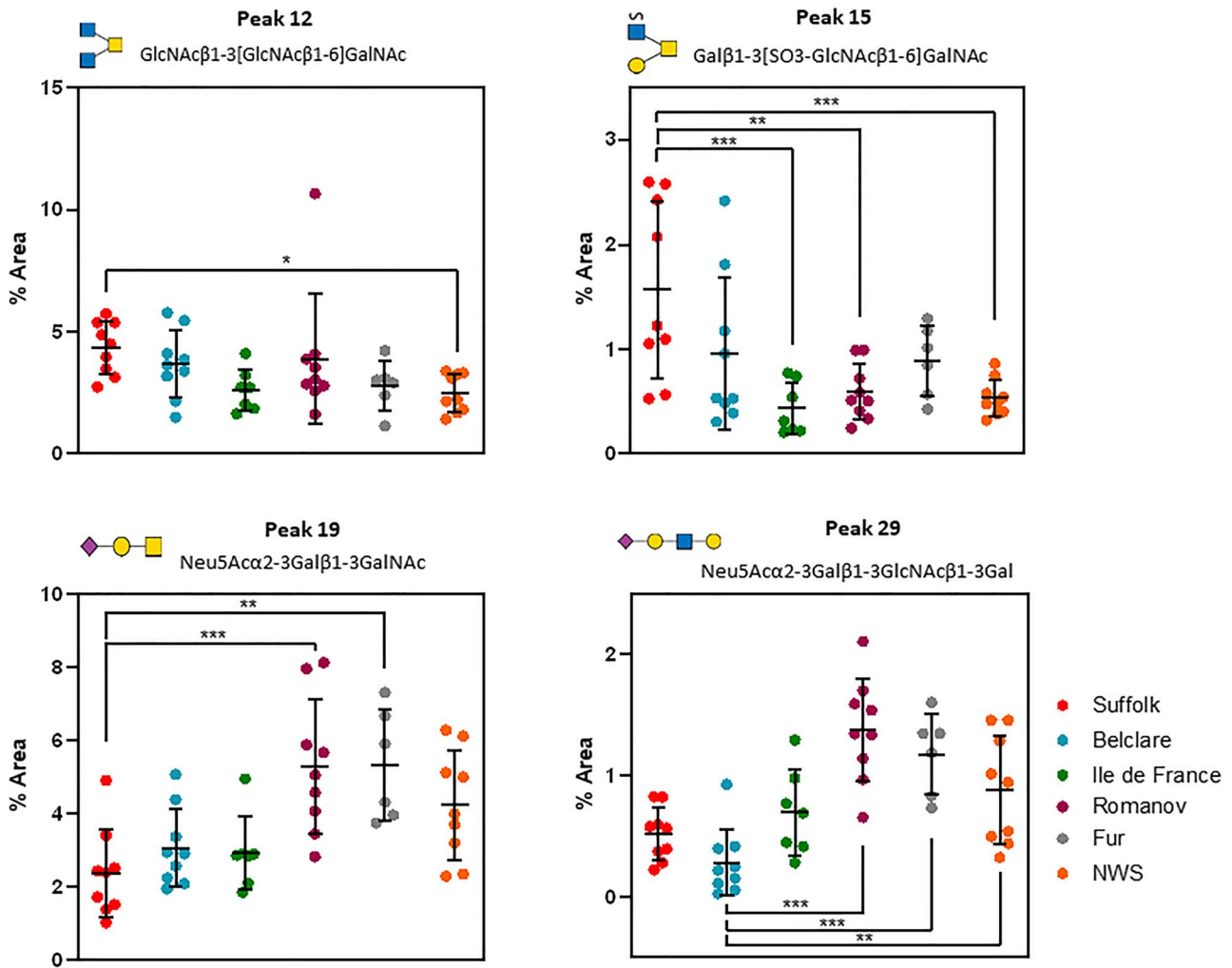
Fig. 3. Nested plots of significantly different *O*-glycans in cervical mucus of six ewe European ewe breeds collected at the follicular phase of a natural cycle. *$P < 0.05$, **$P < 0.01$, ***$P < 0.001$. NWS = Norwegian White Sheep.

Ewe breed differences in cervical mucin *O*-glycans collected at the follicular phase of a natural estrous cycle

Individual glycan peaks and glycan features of six ewe breeds at the natural cycle are presented in Supplementary Tables SXI and SXII, respectively. Regarding individual structures, glycan peaks 1, 4, 10, 12, 15, 16, 17, 19, 20, 21, 22, 29 and 44 were affected by ewe breed ($P < 0.05$; Supplementary Figure S2). Of these, peak 12 (GlcNAcβ1–3[GlcNAcβ1–6]GalNAc) and peak 15 (Galβ1–3[SO3-GlcNAcβ1–6]GalNAc) had higher abundance in Suffolk (low fertility) compared with Norwegian White Sheep (NWS) (highest fertility; $P < 0.05$; Figure 3). Peak 19 (Neu5Acα2–3Galβ1–3GalNAc) also had higher abundance in Suffolk compared with Fur ewes (high fertility; $P < 0.05$). In addition, peak 29 (Neu5Acα2–3Galβ1–3GlcNAcβ1–3Gal) presented lower abundance in Belclare (medium fertility) compared with the Romanov, Fur and NWS ($P < 0.05$). Out of the features assessed, only core 6 glycans had increased expression in Suffolk ($P < 0.001$), Belclare ($P < 0.05$) and Fur ($P < 0.05$) when compared against Ile de France (medium fertility) which presented the lowest abundance of core 6 structures (Figure 4). This was derived only from the expression of a sulfated and
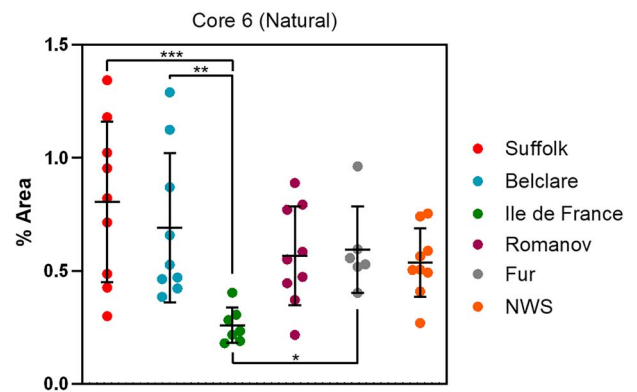

Fig. 4. Nested plot of core 6 glycosylation of cervical mucin from six European ewe breeds at the follicular phase of a natural cycle. *$P < 0.05$, **$P < 0.01$, ***$P < 0.001$. NWS = Norwegian White Sheep.

fucosylated glycan (Galβ1–3(Fucα1–6-SO3-GlcNAcβ1–6)GalNAc) peak 20, which showed higher variation within breed in Suffolk and Belclare compared with the other ewe breeds.
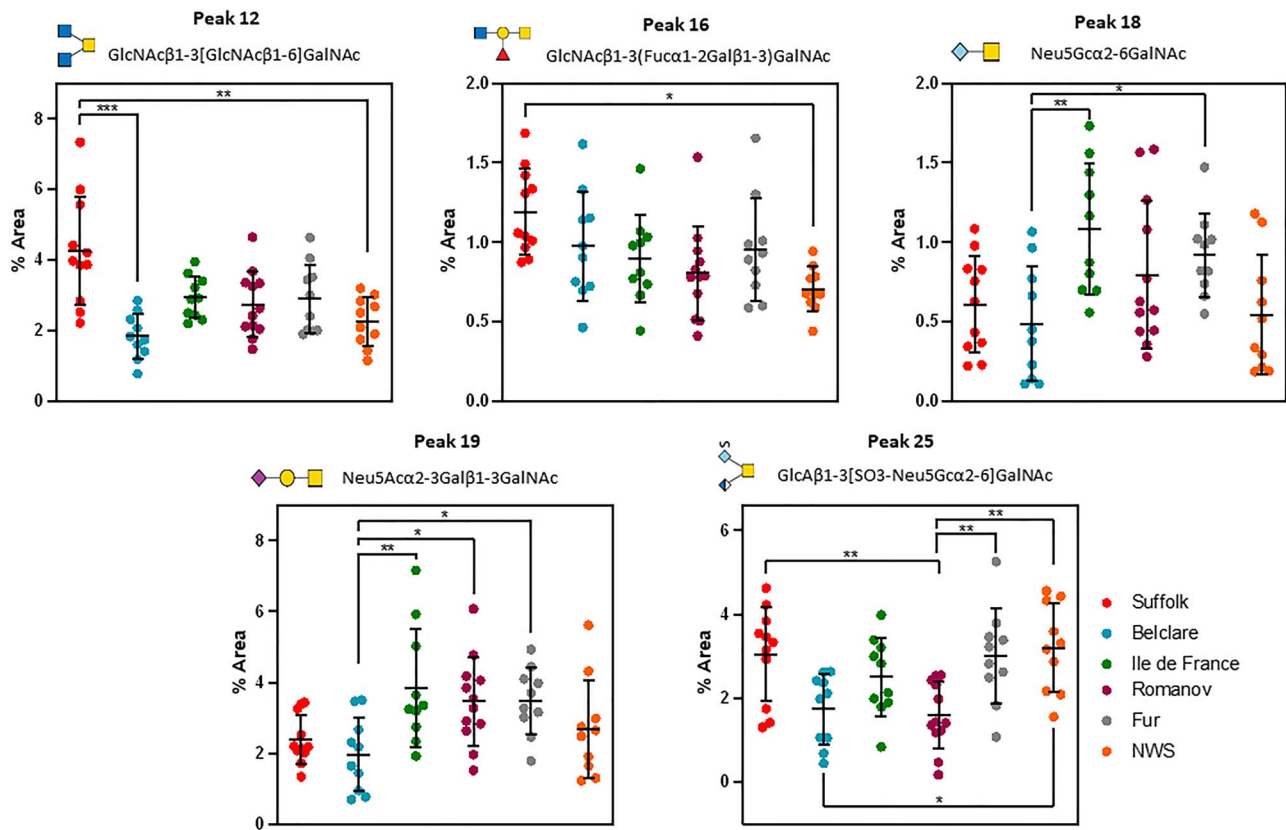
Fig. 5. Nested plots of significantly differentially expressed *O*-glycans in cervical mucus of six European ewe breed collected at the follicular phase of a synchronized cycle. *$P < 0.05$, **$P < 0.01$, ***$P < 0.001$. NWS = Norwegian White Sheep.

Ewe breed differences in cervical mucins *O*-glycans collected at the follicular phase of a synchronized estrous cycle

In the synchronized cycle, glycan peaks 1, 6, 7, 8, 9, 10, 11, 12, 14, 16, 17, 18, 19, 25, 26, 28, 30, 35, 36, 39, 42, 43 and 45 were altered by ewe breed ($P < 0.05$; Supplementary Figure S4 and Supplementary Table SXIII). Of these glycan peaks, peak 12 (GlcNAcβ1–3[GlcNAcβ1–6]GalNAc) and peak 16 (GlcNAcβ1–3(Fucα1-2Galβ1–3)GalNAc) were increased in Suffolk ewes (low fertility) compared with NWS ($P < 0.05$; Figure 5). Peak 18 (Neu5Gcα2–6GalNAc) had lower abundance in Belclare (medium fertility) compared with Ile de France (medium fertility and Fur ewes (high fertility)) ($P < 0.05$). Peak 19 (Neu5Acα2–3Galβ1–3GalNAc) also presented lower abundance in Belclare compared with Ile de France, Romanov and Fur ewes ($P < 0.05$). In addition, peak 25 (GlcAβ1–3[SO3-Neu5Gcα2–6]GalNAc) had lower abundance in Belclare compared with NWS ($P < 0.05$), as well as Romanov (medium fertility) had lower abundance compare with Fur and NWS ($P < 0.05$). However, the abundance of this glycan was higher in Suffolk than in Romanov ewes ($P < 0.05$).

There was a ewe breed by type of cycle interaction in fucosylation, glucuronylation, acetyl-sialylation, core 1 and core 4 ($P < 0.05$), represented by more feature differences between ewe breeds at the synchronized compared with the natural estrous cycle (Supplementary Table SXIV). At a synchronized cycle, fucosylation was increased in Belclare compared with Suffolk ($P < 0.05$). Both Suffolk and NWS had increased glucuronylated structures compared

with the Romanov ($P < 0.05$). Neu5Ac structures were increased in Romanov compared with the Belclare ($P < 0.05$). Core 1 glycans were increased in Ile de France ($P < 0.05$) and Romanov ($P < 0.05$) compared with Belclare. Core 4 glycans were increased in Suffolk compared with Belclare ($P < 0.05$). Dot plots of all significant feature differences are shown in Figure 6. Principal Component Analysis (PCA) was used to compare each breed with the glycans associated with a particular feature, where there were no significant differences (Supplementary Figure S5). However, clear separation was identified between Suffolk and Belclare for core 4 glycans (peaks 12, 41 and 50; Figure 6). In addition, clear separation on PCA plots was also observed between the low-fertility Suffolk and NWS (highest fertility). However, this separation was not significant (Figure 6; $P > 0.05$).

Relationship between mucus viscosity and *O*-glycans

Mucus viscosity was correlated against relative feature and glycan abundance without including peeling peaks (Supplementary Figures S6 and S7). Fucosylation had a positive weak correlation with viscosity ($\rho = 0.27$; $P < 0.05$), whereas core 4 abundance and glucuronylation had a negative weak correlation ($\rho = -0.26$; $P < 0.05$). Glycan peaks 11 (Neu5Acα2–3GalNAc and GlcNAcβ1–3Galβ1–3GalNAc), 24 (Galβ1–3[Galβ1–4GlcNAcβ1–6]GalNAc), 35 (Galα1–3Galβl1–3[Galα1–3GlcNAcβ1–6]GalNAc), 36 (GlcAβ1–3/4galβ1–3[SO3-Neu5Gcα2–6]GalNAc) and 41 (Galβ1–4GlcNAcβ1–3[Galβ1–4(Fucα1–3GlcNAcβ1–6)]GalNAc) were all negatively correlated to mucus viscosity ($\rho = -0.30$, -0.31, -0.29, -0.33 and -0.25, respectively; $P < 0.05$).
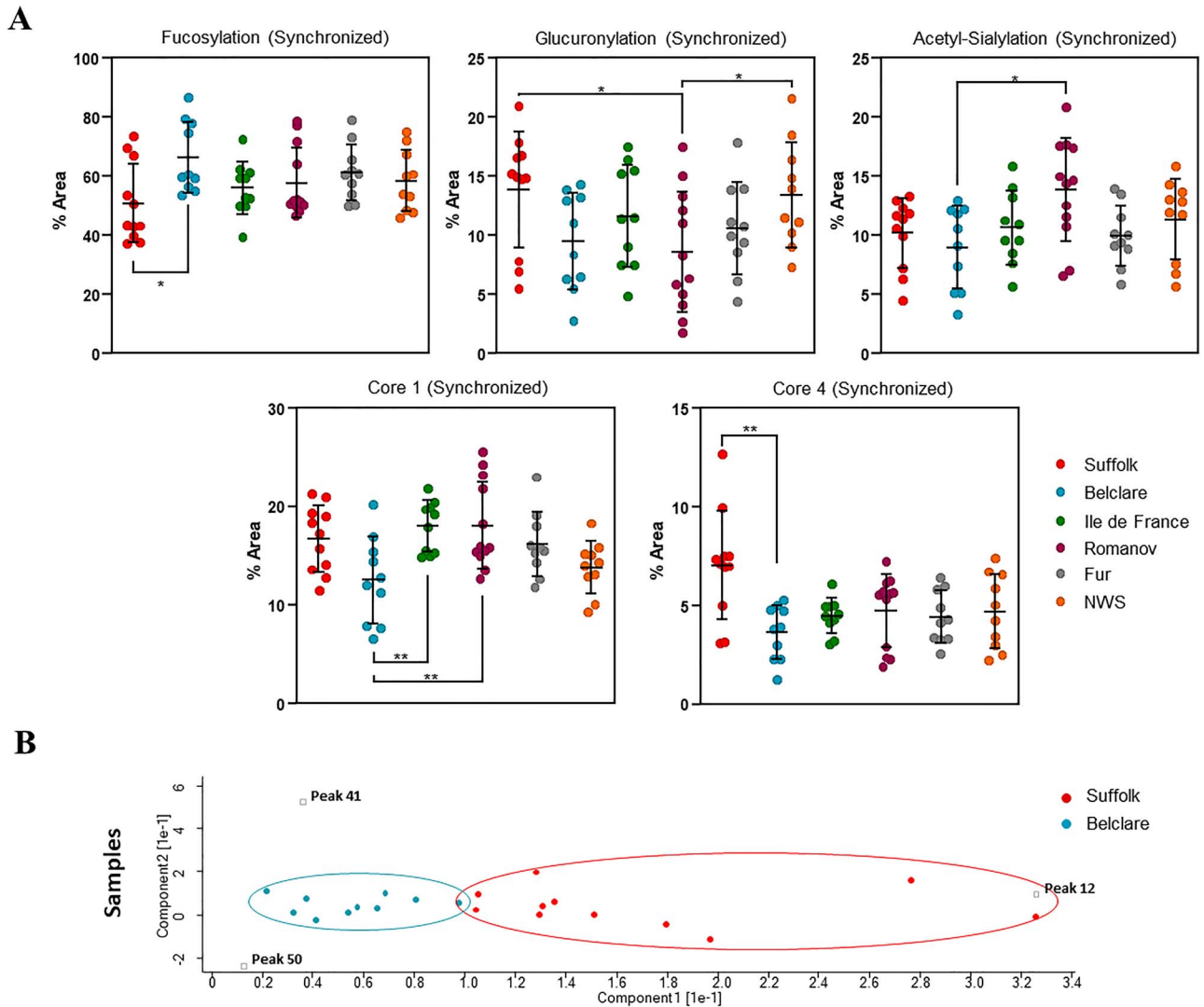
A

B

Fig. 6. (A) Nested plots of significant feature changes (fucosylation, glucuronylation, Neu5Ac, core 1 and core 4) in cervical mucus of six European ewe breeds at the follicular phase of a synchronized cycle. $*P < 0.05$, $**P < 0.01$, $***P < 0.001$. (B) PCA plot shows the three core 4-associated peaks (12, 41 and 50), which are driving the significant difference between Suffolk and Belclare (samples within each breed are indicated by the same colors).

Discussion

This is the first published study that has characterized the O-glycome of sheep cervical mucus. We did this using a novel European model composed of six ewe breeds with known differences in pregnancy rates and cervical sperm transport following cervical AI with frozen–thawed semen. The overall aim was to identify O-glycans as biomarkers of cervical sperm transport. No N-glycans were detected, but we identified significant variations in the profile of O-glycans between high- and low-fertility ewe breeds and between a naturally occurring and hormonally synchronized estrous in some ewe breeds. Results indicate that a core 4 glycan (GlcNAcβ1–3[GlcNAcβ1–6]GalNAc) was related with impaired sperm transport since there was higher abundance in the low-fertility Suffolk breed compared with NWS (highest fertility) at both a natural and a synchronized cycle. In addition, a core 2 sulfated glycan (Galβ1–3[SO3-GlcNAcβ1–6]GalNAc) and a fucosylated glycan (GlcNAcβ1–3(Fucα1–2Galβ1–3)GalNAc) were also increased in Suffolk compared with NWS at the natural and synchronized cycle, respectively.

The first major challenge of this study was to optimize the method developed by Wilkinson et al. (2021) as it is the first time that this method is used for the release of O-glycans from cervical mucin samples. Here, we used a new microwave-assisted β-elimination method, which reduces reaction time in comparison with other chemical methods (reductive β-elimination and nonreductive β-elimination) and also provides comparable yields of released O-glycans, minimizing the peeling products as reviewed by Wilkinson and Saldova (2020).

By combining FLR-HILIC-UPLC, exoglycosidase digestions and ESI-MS, we identified 124 O-glycans across a range of mucin-type cores, from which 51 were the major O-glycans of the cervical mucins. The majority of glycans were core 2 (45%) followed by core 1 (22%). Other cores were also identified, for example, core 6 (11%), core 4 (6%) and core 3 (5.6%). It is well known that core 1 glycans are ubiquitously expressed. In contrast, core 2 glycans are more cell type specific and they act as a scaffold for the production of selectin ligands that act in regulating inflammation. Relatively few tissues

show high levels of core 3 and core 4, except for the gastrointestinal, respiratory tracts and salivary glands, where mucin production is normally high. Thus, core 1–4 glycans represent the most common O-glycan structures produced *in vivo*, with core 2 subtype having the highest abundance as we identified in the present study. Other core structures, such as core 6 glycan also detected in our study, have been previously found on mucins from human embryonic gut and from ovarian cysts (Varki and Schauer 2009).

Our results are in broad agreement with a study of periovulatory cervical mucus of women, which showed T-antigen (core 1 glycan type) having the highest levels around the time of ovulation (Argueso et al. 2002). In our study, T-antigen was one of the 51 major detected O-glycans. In addition, the study demonstrated that those T-antigen glycans were carried by the *MUC5B*, which was increased around the time of ovulation. This suggests that changes in mucin O-glycosylation modulates the mucus rheological properties such as mucus viscosity and water retention capacity and allow sperm to traverse the cervix around the time of ovulation.

In a proteomic study using human cervical mucus from different phases across the estrous cycle, core 2 glycans were found in higher levels around the time of ovulation (Andersch-Bjorkman et al. 2007). In the current study, the levels of neutral glycans such as fucosylated glycans were the most abundant with 56 structures across all six ewe breeds. Analysis of mucus in mouse gastrointestinal tract showed lower sialylation in the stomach compared with the colon (Holmén Larsson et al. 2013), as well as it has been demonstrated that increase sialylation contributes to defense against pathogens in the respiratory tract (Denneny et al. 2020). Cervical mucus rheology and hydration seems to be related to the presence of negatively charged terminal groups on glycoproteins, modifying the distension and flexibility of the mucin protein and increasing mucus viscosity (Varki and Schauer 2009). Taken together, these results indicate that cervical mucus collected from all six ewe breeds at the follicular phase had high abundance of neutral mucins and low proportion of acidic glycans, resulting in a more hydrated and less viscous mucus at the follicular phase. This is supported by previous studies using histochemical and complementary biochemical methods that have also suggested cyclic glycosylation variation over the menstrual cycle due to the variation of hormonal levels, mainly estrogen (Iacobelli et al. 1971; Wakefield and Wells 1985; Argueso et al. 2002).

The use of exogenous hormones to synchronize the estrous cycle had an effect on the O-glycome in some ewe breeds but not others. Although the low-fertility Suffolk breed had higher abundance of the type 3 H-antigen (Fucα1–2Galβ1–3)GalNAc, peak 8) and glucuronyl-Tn-antigen (GlcAβ1–3GalNAc, peak 14) at a natural cycle compared with the synchronized cycle, there was no difference between natural and synchronized estrous in both ewe breeds with the highest fertility (Fur and NWS). The results of this study would suggest that the ewe breed has a significant role in the cervical response to exogenous hormones and could help explain the contradictory results regarding the effect of exogenous hormones in gross mucus properties and sperm transport that have been previously reported. In our previous study (Abril-Parreño et al. 2021), we identified increased mucus production at the synchronized cycle compared with the natural cycle at the follicular phase in all six ewe breeds; however, mucus viscosity did not follow the same trend in all six ewe breeds. Further studies on mucus viscosity have not been performed in this study due to the limited amount of cervical mucus, although the analysis of the addition of sialidases and/or

fucosidases to the cervical mucus and subsequently analysis of mucus viscosity are warranted. This could be due to the insensitivity of the chamber filling method used to assess viscosity in the field. Rexroad Jr and Barb (1977) also reported an increase of mucus production, whereas Smith and Allison (1971) found decreased levels of mucus produced at the synchronized cycle compared with the natural cycle. Maddison et al. (2016) reported similar mucus volumes when Merino ewes were synchronized or not. There have also been reports of changes in Spinnbarkeit (Adams and Tang 1979), protein content (Rexroad Jr and Barb 1977) and reduced fertility in sheep (Crocker et al. 2007) due to the use of exogenous hormones.

Changes in sialylation are widely known to participate in sperm regulation, as sialic acids on highly sialylated beta-defensin 126 is required for human sperm to migrate within the mucin mesh of the cervical mucus (Lyons et al. 2018) and has been shown in the bull to affect sperm motility, ability to penetrate mucus *in vitro* and interaction with the oocyte vestments (Fernandez-Fuertes et al. 2018). However, the role of specific O-glycans from cervical mucin in the selection of sperm is unknown. In the present study, we identified lower abundance of the sialyl-T-antigen (Neu5Acα2–3Galβ1–3GalNAc, peak 19) in the low-fertility Suffolk breed compared with Fur ewes (high fertility) at the natural cycle. At the synchronized cycle, Belclare (medium fertility) had lower abundance of this glycan compared with Fur ewes. The structure (2,3)-sialyl-T-antigen is formed by adding sialic acid to the T-antigen structure, which is antigenic and could represent recognition sites for lectins. This glycan was also identified in the cervical mucus of women (Andersch-Bjorkman et al. 2007), although its role in fertility is unknown.

There are contradictory results regarding the role of sialic acid in the regulation of sperm transport *in vivo*. Lutjen et al. (1985) found decreased terminal sialic acid in infertile patients compared with cervical samples from fertile women. Although other have reported the opposite, a decrease in sialic acid content is related to an increase in mucus receptivity to spermatozoa (Moghissi et al. 1976). In the current study, sialyl-Tn antigen (Neu5Gcα2–6GalNAc, peak 18) was related to fertility, having lower abundance in Belclare ewes (medium fertility) than in Fur ewes (high fertility). However, Richardson et al. (2019) demonstrated increased amounts of Neu5Ac/Neu5Gc α2–6Gal- GalNAc in Suffolk ewes (low fertility) using a lectin assay. This result was associated with low numbers of sperm in the cervical channels of the Suffolk ewes. This suggests that higher levels of sialylated O-glycans in the low-fertility breed are binding sperm and thus inhibiting the sperm progression through the cervix. Specifically, α2,6-linked sialic acid terminal may be involved in the interaction with sialic acid receptors (Siglecs) on the sperm surface, thus causing sperm to become immobilized in the cervical mucins. Sialic acid also plays an important role in the survival of sperm within the female reproductive tract (Crocker et al. 2007), as when sperm are detected an immune response is initiated, which consists of a leukocytic reaction that destroy the majority of the sperm. Specifically, neutrophils are the most abundant immune cell in the human leukocytic reaction following insemination (Thompson et al. 1992). For instance, sialylated cervical mucins seem to silence neutrophils in cows by a sialic acid-dependent mechanism (Bornhöfft et al. 2019). Furthermore, *in vitro* and *in vivo* functional studies are required to understand the precise role of specific sialic acid terminals and Siglecs in cervical sperm transport.
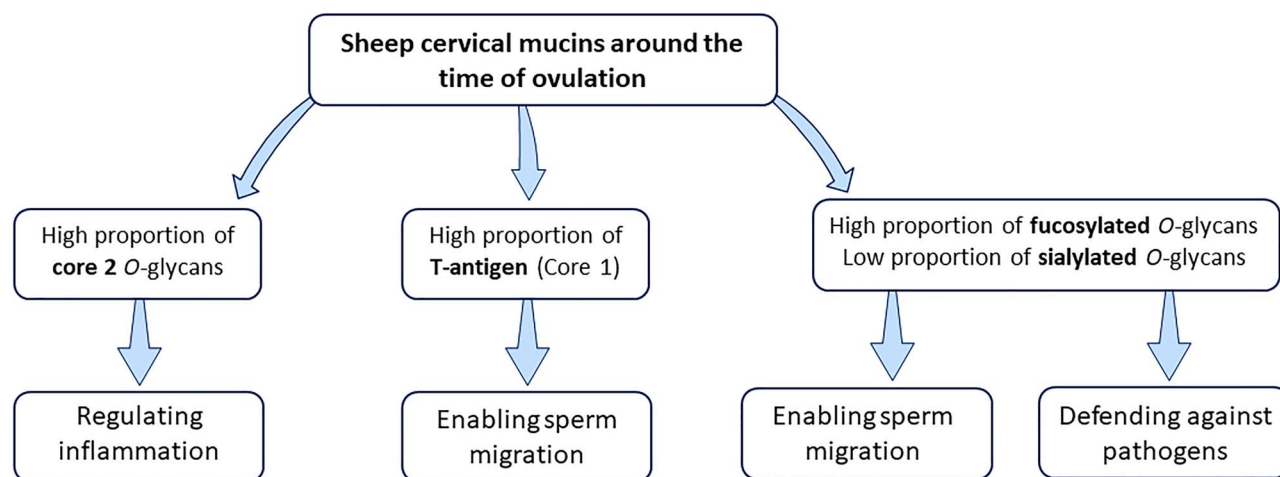
Fig. 7. Overview of the main findings of the characterization of *O*-glycans in cervical mucus across six ewe breeds with divergent fertility at the follicular phase (around the time of ovulation) of the estrous cycle.

It has also been reported that sulfated mucins can inhibit adhesion of bacteria to target gastric cells (Kamisago et al. 1996). In the present study, we identified higher abundance of the sulfated core 2 glycan (Galβ1–3[SO3-GlcNAcβ1–6]GalNAc, peak 15) in the low-fertility Suffolk compared with NWS (highest fertility) at the natural cycle. This suggests that these glycosylation changes may be considered a "side effect" of the presence of bacteria and pathogens. In addition, fucosylated core 1 glycan (GlcNAcβ1–3(Fucα1–2Galβ1–3)GalNAc, peak 16) also had higher abundance in Suffolk compared with NWS ewes (highest fertility) at the synchronized cycle. Fucosylated *O*-glycans mediate ligand adhesion, pathogen–host interactions and cellular processes via signaling mechanisms (Li et al. 2018). It has been reported that cervical mucus with high fucose protect the vaginal epithelial cells against the binding of *Candida albicans* (Domino et al. 2009). It is possible that cervical *O*-glycans bind *C. albicans* in order to avoid binding to epithelial cells. This could explain the role of this fucosylated glycan that was present in higher proportions in the low-fertility ewe breeds as an indicator of an active immune response that could have a negative effect on sperm transport. Core 4 glycan (GlcNAcβ1–3[GlcNAcβ1–6]GalNAc, peak 12), the most abundant peak contributing to the total core 4 glycans, was found in higher abundance in the Suffolk than in the highest fertility ewe breed (NWS) at both the natural and synchronized cycle. Core 4 *O*-GalNAc glycans (as peak 12) have been identified in secreted mucins of some tissues, such as bronchi, colon and salivary glands (Varki and Schauer 2009), but there are no published studies on its role in sperm transport. Although, a transcriptomic analysis of the bovine cervix (Pluta et al. 2012) identified lowest gene expression of the Glucosaminyl (*N*-Acetyl) Transferase 2, which synthetizes the core 4 structures, besides it was correlated with maximal mucin gene expression around the time of ovulation. Therefore, sperm transport can be negatively affected by the high presence of core 4 *O*-glycans. However, we identified a negative correlation with mucus viscosity and core 4 *O*-glycans (between other glycans). Our result supports the essential role of *O*-glycans holding water due to their hydrophilic character and negative charge, which contributes to the viscosity and adhesiveness of mucus (Varki and Schauer 2009). Yet, whether core 4 *O*-glycans contribute to mucin barrier function and how the rheological properties modulate sperm transport through the cervical mucus remain unclear.

In conclusion, this is the first published study of the O-glycome of sheep cervical mucus. We characterized 124 O-glycans, from which 51 were the major glycans with core 2 and fucosylated glycans as the most common structures (Figure 7). Therefore, higher fucosylation and lower sialylation seems to be the optimal environment for the sperm survival in the cervical mucus. We found no differences in the *O*-glycan composition between the synchronized and natural cycle in both high-fertility ewe breeds (NWS and Fur), but there was an effect in the other ewe breeds. Despite no differences in gross mucus properties previously reported by our group (Abril–Parreño et al. 2021), we identified O-glycan changes and potential biomarkers that could be targeted for the improvement of assisted reproduction techniques such as cervical insemination. For example, sulfated glycan (Galβ1–3[SO3-GlcNAcβ1–6]GalNAc), fucosylated glycan (GlcNAcβ1–3(Fucα1–2Galβ1–3)GalNAc) and core 4 glycan (GlcNAcβ1–3[GlcNAcβ1–6]GalNAc), which had higher abundance in the low-fertility Suffolk breed compared with NWS (high fertility). In addition, core 4 glycans were negatively correlated with mucus viscosity. Future *in vitro* and *in vivo* studies using the specific *O*-glycans found in this study are warranted.

Material and methods

Ethical approval

Protocols were developed in accordance with the "Cruelty to Animals Act" (Ireland 1876, as amended by European Communities regulations 2002 and 2005) and the European Community Directive 86/609/EC. In Ireland, the study was approved by the Teagasc Animal Ethics Committee and all animal procedures performed were conducted under experimental license from the Health Products Regulatory Authority. In Norway, the study was approved by Norwegian Food safety Authority (FOTS ID 13168). In France, the study was approved by the ethics committee and the Ministry of Research.

Experimental design

The experimental design has previously been described (Abril-Parreño et al. 2021). Briefly, this study was performed as a part of larger project, which aimed to interrogate the ewe breed differences in cervical mucus properties and anatomical characteristics across

the estrous cycle (at both follicular and luteal phases) of both a synchronized (using progestogen pessaries combined with equine chorionic gonadotropin) and a natural cycle. In this study, we characterized the O-linked glycan composition in the cervical mucus of six ewe breeds (n = 28–30 ewes per breed) across three countries: Ireland (Suffolk and Belclare; low and medium fertility, respectively), France (Ile de France and Romanov; both with medium fertility) and Norway (NWS and Fur; both with high fertility). All the ewes used in this study were multiparous in a range of 4–5 years old. We used these ewe breeds due to their known differences in pregnancy rates following cervical/vaginal AI with frozen–thawed semen. Cervical mucus samples were collected from each ewe at the follicular (around the time of ovulation) of a synchronized (56 h post pessary removal) and a natural estrus cycle (following estrus detection with a teaser ram), which was then replicated three times with the same ewes over a period of ∼6 months. After each mucus collection, samples were transported to the laboratory (within 1 h) and an aliquot assessed for cervical mucus properties (weight, viscosity and color; reported in Abril-Parreño et al. 2021). The remaining sample was stored at −20°C until mucin purification.

Mucin purification from cervical mucus

Mucus samples were ranked according to viscosity at collection (as assessed by the time to fill a 20 μm deep chamber slide) and following thawing were pooled according to viscosity post collection to ensure a sufficient yield of mucins for analysis. Each pool consisted of mucus from five ewes (five most viscous pooled together, then the next five and so on) of the same breed collected over three replicates (total of 15 samples pooled across the five ewes). The volume of mucus in each pool/group was ∼5 mL. Each pooled sample was mixed with an equal volume of 8 M guanidine hydrochloride (GdnCl; Sigma Aldrich, Arklow, Co Wicklow, Ireland) in order to solubilize the mucus and homogenize the samples (the final volume was made up to 30 mL). Dithiothreitol (Sigma Aldrich) was added to a final concentration of 10 mM and incubated at 37°C for 5 h. Iodacetamide (Sigma Aldrich) was added to a final concentration of 25 mM and the samples were incubated at room temperature overnight. The isopycnic density gradient centrifugation was carried out in CsCl/GdnCl. The density of the samples was adjusted to 1.40 g/mL with CsCl in Beckman Ultra-clear tubes, which were centrifuged at 65,000 rpm for 18 h at 10°C in an Optima L-100 XP (Beckman Coulter Inc., Brea, CA) ultracentrifuge using the 70 Ti rotor without break. The density gradient created was unpacked in 1 mL fractions from the top to the bottom of the tube. Following this duplicate, 5 μL aliquots from each fraction were blotted onto a polyvinylidene difluoride membrane using a Whatmann manifold slot blot apparatus (Schleicher & Schuell, Inc., Keene, NH) and stained with periodic acid–Schiff stain (PAS staining; VWR, Radnor, PA) in order to assess the relative intensity of carbohydrate in the sample. The carbohydrate-rich fractions observed from the slot blot, which also had a density profile between 1.35 and 1.45 g/mL, were pooled and then separated by size exclusion chromatography. The samples were loaded on a Sepharose CL-4B column (Sigma Aldrich) and eluted with 50 mM Tris/100 mM KCl, pH 7.5, as mobile phase. The eluate was collected in fractions of 4 mL using a fraction collector, and then a sample (∼20 μL) of all fractions was slot blotted and stained with PAS as described before. Mucin-rich fractions were pooled and freeze-dried, and then resuspended in H_2O and desalted on a Bio-gel P6 column (Bio-Rad Laboratories, Hercules, CA). Fractions collected

with the fraction collector were analyzed by slot blotting and PAS staining (40 μL), and then carbohydrate-rich fractions were pooled and freeze-dried. The freeze-dried material was used as the final pool of purified mucins from each sample and was weighed and stored at −20°C until analysis.

N-glycan release

Purified cervical mucin samples (starting material: 1 mg) were prepared in tubes using the gel method as previously reported (Royle et al. 2008), and N-glycans were released from the glycoproteins by adding PNGase F as previously described (Kuster et al. 1997), following steps were performed using the fractions that only contain O-glycans. N-glycans released were kept for further analysis.

O-glycan release using microwave-assisted nonreductive β-elimination

Our group has recently developed a protocol for the extraction and characterization of O-linked glycans (Wilkinson et al. 2021) with the following modifications. The remaining gels after N-glycan release were crushed by passing them through a small hole in the bottom of a 0.5 mL tube into a 1.5 mL tube at 14,000 rpm and dried down. Then, the crushed gels were resuspended in 250 μL of 40% dimethylamine in water containing 0.1 g/mL ammonium carbonate and transferred to G4 vials (Anton Paar, Graz, Austria). The vials were inserted into a Monowave 450 microwave reactor (Anton Paar), in which the vials were subjected to 20 min microwave radiation at 70°C and 600 W. After the reaction, the remaining solution including the pieces of gel were transferred to 2 mL tubes and neutralized with 1 M HCl (all samples were at pH 7). Samples were desalted using a Hypersep Hypercarb SPE cartridge (Thermo Fisher Scientific, Waltham, MA) and dried.

Reproducibility analysis

First, we determined the viability of the method previously described by Wilkinson et al. (2021), using 1 mg of fetuin glycoprotein (Sigma Aldrich) where the four main O-glycan structures expected in O-glycan release of fetuin were analyzed and presenting a coefficient of variation (CV) below 15%. Then, we validated it for ovine cervical mucin (OCM) by using seven technical replicate release of a randomly selected sample (OCM 37) with all major peaks presenting a CV below 15% (Supplementary Table SI). A total of 72 (in duplicate) cervical mucin samples were analyzed in this study. This comprised of six samples per ewe breed (each was a pool of five ewes), two types of estrous (synchronized and natural) and six ewe breeds.

Glycan labeling with 2-aminobenzamide

The N- and O-glycans released were then fluorescently labeled through reductive amination where the aldehyde group of the reducing glycans undergo a condensation reaction with an aromatic amine in excess to drive the formation of a Schiff base. The aromatic amine label used in this study was 2-aminobenzamide (2AB) (Bigge et al. 1995). After the incubation with 1% formic acid for 40 min at room temperature, 2AB labeling mixture was added and incubated at 65°C for 2 h. Excess label was removed using a Hypersep Diol SPE cartridge (Thermo Fisher Scientific) (Adamczyk et al. 2017).

UPLC analysis of 2AB-labeled glycans

The 2AB-labeled O-glycans were separated by UPLC analysis using a Glycan BEH Amide, 130 Å, 1.7 μm column (Waters Corporation, Milford, MA) on an Aquity H-Class HILIC-UPLC system (Waters Corporation) coupled with a fluorescence detector (Waters Corporation). Solvent A was 50 mM ammonium formate, prepared with 50 mM formic acid, adjusted to pH 4.4 with ammonium hydroxide solution, and solvent B was acetonitrile (ACN). The column temperature was set to 40°C. Nonreductive β-eliminated 2AB-labeled O-glycans were resuspended in 20 μL 88% ACN, and an injection volume of 19 μL was used in a flow rate of 561 μL/min over a 30 min run using the following gradient: 0.00–1.47 min, 12% A; 1.47–25.00 min, 12% → 47.6% A; 25.00–25.60 min, 47.6% → 70% A (flow rate 300 μL/min); 25.60–26.80 min, 70% A (flow rate 300 μL/min); 26.80–28.00 min, 70% → 12% A (flow rate 300 μL/min); 28.00–30.00 min, 12% A (flow rate 561 μL/min). The separation temperature was set at 40°C, whereas the sample temperature was 5°C. Excitation and emission wavelengths for fluorescence detection were λ = 330 nm and λ = 420 nm, respectively. External calibration was performed using 2AB-labeled glucose oligomers, creating a dextran ladder with retention times of all identified glycan peaks expressed in glucose units. The 2AB-labeled N-glycans were also analyzed by UPLC using the method described by Saldova et al. (2014). No N-glycans were found in the cervical mucus samples, and the further analysis was only performed using O-glycans.

Mass spectrometry

Prior to analysis, the 2AB-labeled O-glycans were desalted using 10 μL normal phase Phytip® Columns (Phynexus Inc., San Jose, CA). The 2AB-labeled O-glycans were resuspended in 10 μL 88% ACN, and 9 μL was injected into an Aquity H-Class HILIC-UPLC system (Waters Corporation) with a BEH Glycan column (1.0 × 150 mm, 1.7 μm particle size; Waters Corporation) and an AQUITY fluorescence detector coupled in line with a Waters Xevo G2 QTof system (Waters Corporation). The flow rate was 150 μL/min and the column temperature was set to 60°C. Solvent A was 50 mM ammonium formate, prepared with 50 mM formic acid, adjusted to pH 4.4 with ammonium hydroxide solution, and solvent B was ACN. The oligosaccharides were eluted over a 30 min run using the following gradient: 0.00–1.00 min, 12% A; 1.00–25.00 min, 12% → 47% A; 25.00–25.50 min, 47% → 70% A; 25.50–25.55 min, 70% A (flow rate 100 μL/min); 25.55–26.50 min, 70% A (flow rate 100 μL/min); 26.50–27.00 min, 70% → 12% A (flow rate 100 μL/min); 27.00–30.00 min, 12% A (flow rate 150 μL/min). Excitation and emission wavelengths for fluorescence detection were λ = 330 nm and λ = 420 nm, respectively. The instrument was operated in negative ion sensitivity mode with a capillary voltage of 1.80 kV. The ion source block and nitrogen desolvation gas temperatures were set at 120 and 400°C, respectively. The desolvation gas was set to a flow rate of 600 L/h. The cone voltage was maintained at 50 V. Full-scan data for glycans were acquired over m/z range of 450–2500. The data were collected and processed using MassLynx 4.1 software (Waters Corporation).

Exoglycosidase digestions

Exoglycosidase digestions were undertaken to determine the O-glycan sequence and linkage as has been previously described (Saldova et al. 2014). All enzymes were from New England Biolabs (Hitchin, Herts, UK) except for NAN1, which was purchased from

Prozyme (San Leandro, CA). The 2AB-labeled O-glycans were incubated in a volume of 10 μL for 18 h at 37°C in 50 mM sodium acetate buffer, pH 5.5. An array of the following enzymes was used: sialidase cloned from *Streptococcus pneumoniae* and expressed in *Escherichia coli* (NAN1, EC 3.2.1.18), 5 U/mL; sialidase cloned from *Arthrobacter ureafaciens* and expressed in *E. coli* (ABS, EC 3.2.1.18), 1000 U/mL; β-galactosidase cloned from bovine testis and expressed in *Pichia pastoris* (BTG, EC 3.2.1.23), 200 U/mL; β-galactosidase cloned from *S. pneumoniae* and expressed in *E. coli* (SPG, EC 3.2.1.23), 80 U/mL; α-fucosidase cloned from bovine kidney and expressed in *E. coli* (BKF, EC 3.2.1.51), 800 U/mL; β-N-acetylglucosaminidase cloned from *S. pneumoniae* and expressed in *E. coli* (GUH, EC 3.2.1.30), 400 U/mL; α-mannosidase cloned from *Canavalia ensiformis* (Jack Bean) and expressed in *P. pastoris* (JBM, EC 3.2.1.24), 400 U/mL; α-fucosidase cloned from the sweet almond tree (*Prunus dulcis*) and expressed in *P. pastoris* (AMF, EC 3.2.1.111), 400 U/mL; β-N-acetylhexosaminidase cloned from *Streptomyces plicatus* and overexpressed in *E. coli* (JBH, EC 3.2.1.52), 800 U/mL; and α-galactosidase cloned from green coffee bean and expressed in *E. coli* (CBG, EC 3.2.1.22), 800 U/mL.

Glycan identification and data validation

First, chromatograms from the HILIC-UPLC analysis were separated into peaks. Each peak is composed of one or more O-glycans, of which some could have the same retention time or mass. To separate these glycans, combination of exoglycosidase digestions was used to elucidate the different structures within each peak, since the structural analysis of O-glycans involves not only monosaccharide composition, but also the type of linkages. HILIC-UPLC and exoglycosidase digestions analysis was complemented by mass spectrometry data to fully assign and confirm the presence of these glycan structures (Supplementary Figure S8).

Statistical analysis

Glycan Analysis. The UPLC profiles were separated into peaks and the area under each glycan peak was expressed as a relative percentage area derived from the UPLC total profile. Thus, the logit transformed value was used to map the data onto a more Gaussian distribution as previously described by Saldova et al. (2014). Peak data were checked for normal distribution using a Kolmogorov–Smirnov nonparametric test. Multivariate analysis of variance with post hoc analysis using Tukey's Honest Significant difference test was then performed using SPSS software (IBM Corp., Armonk, NY) to identify significant peak differences across groups. The pool of mucus was the experimental unit and the model included fixed effects for ewe breed, type of cycle (synchronized and natural) and their interaction.

Feature Analysis. Glycan peaks were pooled based on similar structural features (core 1–4, core 6, fucosylated, sialylated, glucuronylated and sulfated). Features pertaining to a peak were determined based on the major glycan members of that peak. See Supplementary Table SIII, where all glycans in all peaks are described, including their amount and peaks included in a particular feature are highlighted in red. We performed statistical analysis on features, as described above.

Viscosity Analysis. A Spearman correlation was performed to assess the relationship between O-glycan profile and mucus viscosity. The comparisons were considered statistically significant when $P < 0.05$.

Supplementary data

Supplementary data for this article is available online at http://glycob.oxfordjournals.org/.

Authors' Contribution

L.A.-P., X.D. and A.K. collected the samples from the ewes. L.A.-P. performed the mucin purifications, the *O*-glycan characterization and drafted the manuscript. S.F., A.K and X.D conceived and designed the experimental model and secured funding. R.S. designed the glycomic analysis. M.E.G. and C.R. facilitated the mucin purification. L.A.-P., H.W., J.M. and R.S. performed the glycomic data analysis. All authors proof read the manuscript.

Conflict of Interest

None declared.

Abbreviations

2AB, 2-aminobenzamide; ACN, acetonitrile; AI, artificial insemination; CV, coefficient of variation; ESI-MS, electrospray ionization mass spectrometry; FLR-HILIC-UPLC, fluorescence hydrophilic interaction ultrahigh-performance liquid chromatography; Fuc, fucose; Gal, galactose; GalNAc, *N*-acetylgalactosamine; GdnCl, guanidine hydrochloride; GlcA, glucuronic acid; GlcNAc, *N*-acetylglucosamine; NWS, Norwegian White Sheep; OCM, ovine cervical mucin; PAS, periodic acid–Schiff; PCA, principal component analysis

References

Abril-Parreño L, Krogenaes AK, Byrne CJ, Donovan A, Stuen S, Caldas E, Diskin M, Druart X, Fair S. 2020. Ewe breed differences in cervical anatomy and cervicovaginal mucus properties: An international study. *Theriogenology*. 160:18–25.

Abril-Parreño L, Krogenæs AK, Byrne CJ, Donovan A, Stuen S, Caldas E, Diskin M, Druart X, Fair S. 2021. Ewe breed differences in cervical anatomy and cervicovaginal mucus properties: An international study. *Theriogenology*. 160:18–25.

Adamczyk B, Stockmann H, O'Flaherty R, Karlsson NG, Rudd PM. 2017. High-throughput analysis of the plasma N-glycome by UHPLC. *Methods Mol Biol*. 1503:97–108.

Adams NR, Tang BY. 1979. Changes in ovine cervical mucus in response to oestrogen treatment. *J Reprod Fertil*. 57:261–266.

Andersch-Bjorkman Y, Thomsson KA, Holmen Larsson JM, Ekerhovd E, Hansson GC. 2007. Large scale identification of proteins, mucins, and their O-glycosylation in the endocervical mucus during the menstrual cycle. *Mol Cell Proteomics*. 6:708–716.

Argueso P, Spurr-Michaud S, Tisdale A, Gipson IK. 2002. Variation in the amount of T antigen and N-acetyllactosamine oligosaccharides in human cervical mucus secretions with the menstrual cycle. *J Clin Endocrinol Metab*. 87:5641–5648.

Bigge JC, Patel TP, Bruce JA, Goulding PN, Charles SM, Parekh RB. 1995. Nonselective and efficient fluorescent labeling of glycans using 2-amino benzamide and anthranilic acid. *Anal Biochem*. 230:229–238.

Bornhöfft KF, Rebl A, Gallagher ME, Viergutz T, Zlatina K, Reid C, Galuska SP. 2019. Sialylated cervical mucins inhibit the activation of neutrophils to form neutrophil extracellular traps in bovine in vitro model. *Front Immunol*. 10:2478.

Brunelli R, Papi M, Arcovito G, Bompiani A, Castagnola M, Parasassi T, Sampaolese B, Vincenzoni F, De Spirito M. 2007. Globular structure of human ovulatory cervical mucus. *FASEB J*. 21:3872–3876.

Corfield AP. 2015. Mucins: A biologically relevant glycan barrier in mucosal protection. *Biochim Biophys Acta*. 1850:236–252.

Crocker PR, Paulson JC, Varki A. 2007. Siglecs and their roles in the immune system. *Nat Rev Immunol*. 7:255–266.

Denneny E, Sahota J, Beatson R, Thornton D, Burchell J, Porter J. 2020. Mucins and their receptors in chronic lung disease. *Clin Transl Immunol*. 9:e01120.

Domino SE, Hurd EA, Thomsson KA, Karnak DM, Holmén Larsson JM, Thomsson E, Bäckström M, Hansson GC. 2009. Cervical mucins carry alpha(1,2)fucosylated glycans that partly protect from experimental vaginal candidiasis. *Glycoconj J*. 26:1125–1134.

Donovan A, Hanrahan JP, Kummen E, Duffy P, Boland MP. 2004. Fertility in the ewe following cervical insemination with fresh or frozen-thawed semen at a natural or synchronised oestrus. *Anim Reprod Sci*. 84:359–368.

Fair S, Hanrahan JP, Donovan A, Duffy P, O'Meara CM, Lonergan P, Evans AC. 2007. Hormonal relationships during the periovulatory period among ewe breeds known to differ in fertility after cervical artificial insemination with frozen thawed semen. *Anim Reprod Sci*. 97:284–294.

Fair S, Hanrahan JP, O'Meara CM, Duffy P, Rizos D, Wade M, Donovan A, Boland MP, Lonergan P, Evans AC. 2005. Differences between Belclare and Suffolk ewes in fertilization rate, embryo quality and accessory sperm number after cervical or laparoscopic artificial insemination. *Theriogenology*. 63:1995–2005.

Fair S, Meade KG, Reynaud K, Druart X, de Graaf SP. 2019. The biological mechanisms regulating sperm selection by the ovine cervix. *Reproduction*. 158:R1–R13.

Fernandez-Fuertes B, Blanco-Fernandez A, Reid CJ, Meade KG, Fair S, Lonergan P. 2018. Removal of sialic acid from bull sperm decreases motility and mucus penetration ability but increases zona pellucida binding and polyspermic penetration in vitro. *Reproduction*. 155:481–492.

Gipson IK. 2001. Mucins of the human endocervix. *Front Biosci*. 6:D1245–D1255.

Gipson IK, Moccia R, Spurr-Michaud S, Argueso P, Gargiulo AR, Hill JA 3rd, Offner GD, Keutmann HT. 2001. The amount of MUC5B mucin in cervical mucus peaks at midcycle. *J Clin Endocrinol Metab*. 86:594–600.

Holmén Larsson JM, Thomsson KA, Rodríguez-Piñeiro AM, Karlsson H, Hansson GC. 2013. Studies of mucus in mouse stomach, small intestine, and colon. III. Gastrointestinal Muc5ac and Muc2 mucin O-glycan patterns reveal a regiospecific distribution. *Am J Physiol Gastrointest Liver Physiol*. 305:G357–G363.

Iacobelli S, Garcea N, Angeloni C. 1971. Biochemistry of cervical mucus: A comparative analysis of the secretion from preovulatory, postovulatory, and pregnancy periods. *Fertil Steril*. 22:727–734.

Kamisago S, Iwamori M, Tai T, Mitamura K, Yazaki Y, Sugano K. 1996. Role of sulfatides in adhesion of Helicobacter pylori to gastric cancer cells. *Infect Immun*. 64:624–628.

Katz DF, Overstreet JW, Hanson FW. 1980. A new quantitative test for sperm penetration into cervical mucus. *Fertil Steril*. 33:179–186.

Kuster B, Wheeler SF, Hunter AP, Dwek RA, Harvey DJ. 1997. Sequencing of N-linked oligosaccharides directly from protein gels: In-gel deglycosylation followed by matrix-assisted laser desorption/ionization mass spectrometry and normal-phase high-performance liquid chromatography. *Anal Biochem*. 250:82–101.

Lagow E, DeSouza MM, Carson DD. 1999. Mammalian reproductive tract mucins. *Hum Reprod Update*. 5:280–292.

Lai SK, Wang YY, Cone R, Wirtz D, Hanes J. 2009. Altering mucus rheology to "solidify" human mucus at the nanoscale. *PLoS One*. 4:e4294.

Li J, Hsu H-C, Mountz JD, Allen JG. 2018. Unmasking fucosylation: From cell adhesion to immune system regulation and diseases. *Cell Chem Biol*. 25:499–512.

Lutjen PJ, Handley CJ, de Witt MT, Trounson AO, McBain JC. 1985. Biochemical changes in cervical mucus-factor infertility. *Gamete Res*. 12:265–274.

Lyons A, Narciandi F, Donnellan E, Romero-Aguirregomezcorta J, Farrelly CO, Lonergan P, Meade KG, Fair S. 2018. Recombinant *β*-defensin 126 promotes bull sperm binding to bovine oviductal epithelia. *Reprod Fertil Dev*. 30:1472–1481.

Ma X, Pan Q, Feng Y, Choudhury BP, Ma Q, Gagneux P, Ma F. 2016. Sialylation facilitates the maturation of mammalian sperm and affects its survival in female uterus. *Biol Reprod*. 94:123.

Maddison JW, Rickard JP, Mooney E, Bernecic NC, Soleilhavoup C, Tsikis G, Druart X, Leahy T, de Graaf SP. 2016. Oestrus synchronisation and superovulation alter the production and biochemical constituents of ovine cervicovaginal mucus. *Anim Reprod Sci*. 172:114–122.

Marczynski M, Balzer BN, Jiang K, Lutz TM, Crouzier T, Lieleg O. 2020. Charged glycan residues critically contribute to the adsorption and lubricity of mucins. *Colloids Surf B Biointerfaces*. 187:110614.

Moghissi KS, Syner FN, Borin B. 1976. Cyclic changes of cervical mucus enzymes related to the time of ovulation. I. Alkaline phosphatase. *Am J Obstet Gynecol*. 125:1044–1048.

Paulenz H, Soderquist L, Adnoy T, Nordstoga AB, Andersen BK. 2005. Effect of vaginal and cervical deposition of semen on the fertility of sheep inseminated with frozen-thawed semen. *Vet Rec*. 156:372–375.

Pluta K, PA MG, Reid CJ, Browne JA, Irwin JA, Tharmalingam T, Corfield A, Baird A, Loftus BJ, Evans AC, et al. 2012. Molecular aspects of mucin biosynthesis and mucus formation in the bovine cervix during the periestrous period. *Physiol Genomics*. 44:1165–1178.

Ragni G, Di Pietro R, Bestetti O, De Lauretis L, Olivares D, Guercilena S. 1985. Morphological selection of human spermatozoa in cervical mucus "in vivo". *Andrologia*. 17:508–512.

Rexroad CE Jr, Barb CR. 1977. Cervical mucus in estrous ewes after treatment with estrogen, progestogens and intrauterine devices. *J Anim Sci*. 44:102–105.

Richardson L, Hanrahan JP, Tharmalingam T, Carrington SD, Lonergan P, Evans ACO, Fair S. 2019. Cervical mucus sialic acid content determines the ability of frozen-thawed ram sperm to migrate through the cervix. *Reproduction*. 157:259–271.

Royle L, Campbell MP, Radcliffe CM, White DM, Harvey DJ, Abrahams JL, Kim YG, Henry GW, Shadick NA, Weinblatt ME, et al. 2008. HPLC-based analysis of serum N-glycans on a 96-well plate platform with dedicated database software. *Anal Biochem*. 376:1–12.

Saldova R, Asadi Shehni A, Haakensen VD, Steinfeld I, Hilliard M, Kifer I, Helland A, Yakhini Z, Borresen-Dale AL, Rudd PM. 2014. Association of N-glycosylation with breast carcinoma and systemic features using high-resolution quantitative UPLC. *J Proteome Res*. 13: 2314–2327.

Smith JF, Allison AJ. 1971. The effect of exogenous progestagen on the production of cervical mucus in the ewe. *Reproduction*. 24:279.

Tecle E, Gagneux P. 2015. Sugar-coated sperm: Unraveling the functions of the mammalian sperm glycocalyx. *Mol Reprod Dev*. 82:635–650.

Thompson LA, Barratt CLR, Bolton AE, Cooke ID. 1992. The leukocytic reaction of the human uterine cervix. *Am J Reprod Immunol*. 28:85–89.

Varki A, Schauer R. 2009. Sialic acids. In: Varki A, Cummings RD, Esko JD, Freeze HH, Stanley P, Bertozzi CR, Hart GW, Etzler ME, editors. *Essentials of glycobiology*. Cold Spring Harbor (NY): Cold Spring Harbor Laboratory Press Copyright © 2009, The Consortium of Glycobiology Editors, La Jolla, California.

Wakefield EA, Wells M. 1985. Histochemical study of endocervical glycoproteins throughout the normal menstrual cycle and adjacent to cervical intraepithelial neoplasia. *Int J Gynecol Pathol*. 4:230–239.

Wilkinson H, Saldova R. 2020. Current methods for the characterization of O-glycans. *J Proteome Res*. 19:3890–3905.

Wilkinson H, Thomsson KA, Rebelo AL, Hilliard M, Pandit A, Rudd PM, Karlsson NG, Saldova R. 2021. The O-glycome of human nigrostriatal tissue and its alteration in Parkinson's disease. *J Proteome Res*. 20(8):3913–3924.